



Vibration analysis of rectangular plates with edge V-notches

C.S. Huang^{a,*}, A.W. Leissa^b, S.C. Liao^a

^a Department of Civil Engineering, National Chiao Tung University, 1001 Ta-Hsueh Road, Hsinchu, Taiwan

^b Department of Mechanical Engineering, Colorado State University, Fort Collins, CO 80523, USA

ARTICLE INFO

Article history:

Received 20 November 2007

Received in revised form

21 February 2008

Accepted 25 May 2008

Available online 29 May 2008

Keywords:

Ritz method

Thin plate

Vibration

V-notch

Stress singularity

ABSTRACT

A method is presented for accurately determining the natural frequencies of plates having V-notches along their edges. It is based on the Ritz method and utilizes two sets of admissible functions simultaneously, which are (1) algebraic polynomials from a mathematically complete set of functions, and (2) corner functions duplicating the boundary conditions along the edges of the notch, and describing the stress singularities at its sharp vertex exactly. The method is demonstrated for free, square plates with a single V-notch. The effects of corner functions on the convergence of solutions are shown through comprehensive convergence studies. The corner functions accelerate convergence of results significantly. Accurate numerical results for free vibration frequencies and nodal patterns are tabulated for V-notched square plates having notch angle $\alpha = 5^\circ$ or 30° at different locations and with various notch depths. These are the first known frequency and nodal pattern results available in the published literature for rectangular plates with V-notches.

© 2008 Elsevier Ltd. All rights reserved.

1. Introduction

Plates are widely used as structural elements throughout engineering designs. Their vibrational behavior is of great interest, especially the free vibration characteristics (natural frequencies and their corresponding mode shapes). At least 2000 research papers have been published on this topic. In his monograph on the subject, Leissa [1] summarized the methods of analysis and numerical results found in 500 references on the free vibration of plates published before 1967. Since then, research and publication on this subject has been at an increasing rate.

Among all the possible shapes of plates (rectangular, circular, triangular, trapezoidal, etc.), the rectangular plate is of the greatest importance and interest in vibration analysis. Approximately half of the 500 papers and reports described in Leissa's monograph were devoted to rectangular plates, and this appears to be the case also for the numerous subsequent publications on plate vibrations. There have been some vibration analyses of rectangular plates having interior cutouts or holes (e.g., rectangular or circular), and cracks or slits (internal or external). But, the writers have found no publications that consider the effects of an edge V-notch (Fig. 1). Such notches can appear, perhaps cut intentionally in the plate for clearance or other reasons. The interesting questions arise "What is the effect of an edge V-notch

on plate frequencies and mode shapes? Can a shallow notch cause significant changes in them?"

The present work demonstrates a method for analyzing the free vibrations of plates with V-notches. It is presented in detail for rectangular plates having a single V-notch, although it can be used straightforwardly for other shapes of plates and in situations where there is more than one V-notch on the periphery. The method uses two types of functions simultaneously to describe the transverse displacement of the plate during its vibrations: (1) algebraic polynomials, which can form a complete set of functions, and (2) corner functions, which duplicate the boundary conditions along the edges of the notch, and describe the stress singularities at its sharp vertex exactly. These two sets of functions are used with the well-known Ritz method to obtain accurate frequencies and mode shapes. The stress singularities at sharp corners were first investigated by Williams [2], who demonstrated the singularities and their strengths, and also found the corresponding displacement eigenfunctions. These eigenfunctions, which we call "corner functions", were used, along with suitable polynomials, to obtain accurate vibration frequencies and mode shapes for sectorial plates [3] and circular plates with V-notches [4].

The Ritz method is more suitable than a traditional finite element approach for determining the natural frequencies and mode shapes of thin plates with V-notches. The geometry of the plate shown in Fig. 2 is quite simple, so that the area integration used in the Ritz method is easy to set up. Based on the classical thin plate theory, a finite element approach needs C^1 type elements that are much more complicated than C^0 type elements

* Corresponding author. Tel.: +886 3 5712121.

E-mail address: cshuang@mail.nctu.edu.tw (C.S. Huang).

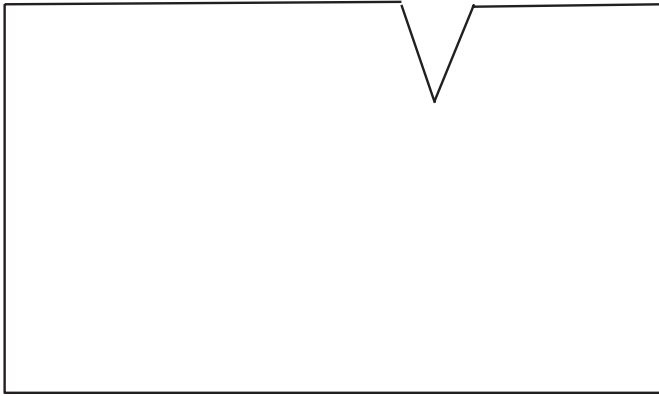


Fig. 1. Rectangular plate with an edge V-notch.

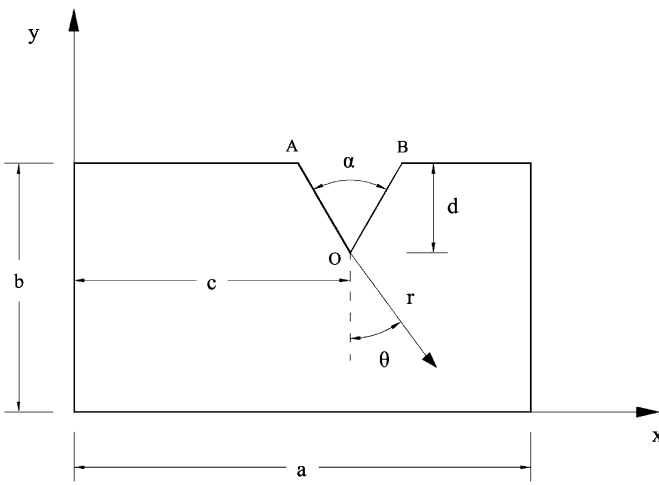


Fig. 2. Dimensions and coordinates for a V-notched plate.

and are usually unavailable in a commercial finite element computer program. If the first-order shear deformation plate theory is used to analyze a thin plate problem in a finite element approach, then the shear locking problem can be anticipated.

The analysis method for rectangular plates with edge V-notches is laid out in the present work for arbitrary edge constraints (i.e., clamped, simply supported or free). It is demonstrated here by obtaining extensive results for frequencies and mode shapes of free, square plates having various notch angles (α), depths (d) and locations (c), described in Fig. 2. The excellent accuracy of the results is shown by several tables of convergence studies.

2. Analysis

The thin plate under consideration is a rectangular plate with a V-notch whose vertex (notch) angle is α as shown in Fig. 2. In the Ritz method, the maximum strain energy (V_{max}) and the maximum kinetic energy (T_{max}) for a plate vibrating harmonically with amplitude $W(x, y)$ and circular frequency ω are the area integrals [1]:

$$V_{max} = \frac{D}{2} \int \int_A [(W_{,xx} + W_{,yy})^2 - 2(1 - \nu)(W_{,xx}W_{,yy} - (W_{,xy})^2)] dA, \tag{1a}$$

$$T_{max} = \frac{\omega^2 \rho}{2} \int \int_A W^2 dA, \tag{1b}$$

where D , ν and ρ are the flexural rigidity of the plate, Poisson's ratio and mass per unit area, respectively; and the subscript comma denotes partial differentiation with respect to the coordinates defined by the variables after the comma. The vibration frequencies of the plate are obtained by minimizing the energy functional

$$\Pi = V_{max} - T_{max}. \tag{2}$$

The admissible functions of the Ritz method must satisfy the essential (i.e., geometrical) boundary conditions of the problem under consideration. For a rectangular plate with a V-notch shown in Fig. 2, the area integrations in Eqs. (1a and b) are easy to perform in the Cartesian coordinate system. The admissible functions for the transverse displacement are assumed as the sum of two sets of functions:

$$W(x, y) = x^l y^m (x - a)^n (y - b)^q [W_p(x, y) + W_c(r, \theta)], \tag{3}$$

where $W_p(x, y)$ consists of algebraic polynomials and is expressed as

$$W_p(x, y) = \sum_{i=0,1}^{l-1} \sum_{j=0,1}^{m-1} a_{ij} x^i y^j \tag{4}$$

and $W_c(r, \theta)$ consists of corner functions that accurately describe the singular behaviors at the vertex of a V-notch and also satisfy the natural boundary conditions (i.e., zero bending moment and effective shear force along the two edges of the V-notch).

In Eq. (3) l is 0, 1 or 2, depending upon whether the edge $x = 0$ is free, simply supported or clamped, respectively. Similarly, choosing m , n and q either 0, 1 or 2 will result in the other edges being free, simply supported or clamped.

Following the solution procedure given in Williams [2], which showed the stress singularities occurring at the tip of a V-notch when $\alpha < 180^\circ$, one can find the corner functions W_c for a corner with two free edges expressed as

$$W_{cn}^S(r, \theta) = r^{\lambda_n+1} \left[\frac{\gamma_2 \sin[(\lambda_n - 1)\beta/2]}{\gamma_1 \sin[(\lambda_n + 1)\beta/2]} \cos(\lambda_n + 1)\theta + \cos(\lambda_n - 1)\theta \right], \tag{5a}$$

$$W_{cn}^A(r, \theta) = r^{\bar{\lambda}_n+1} \left[\frac{\bar{\gamma}_2 \cos[(\bar{\lambda}_n - 1)\beta/2]}{\bar{\gamma}_1 \cos[(\bar{\lambda}_n + 1)\beta/2]} \sin(\bar{\lambda}_n + 1)\theta + \sin(\bar{\lambda}_n - 1)\theta \right], \tag{5b}$$

where $\gamma_1 = (\lambda_n+1)(\nu-1)$, $\gamma_2 = -\lambda_n(\nu-1)+3+\nu$, $\bar{\gamma}_1 = (\bar{\lambda}_n+1)(\nu-1)$, $\bar{\gamma}_2 = -\bar{\lambda}_n(\nu-1)+3+\nu$, $\beta = 2\pi-\alpha$ and λ_n and $\bar{\lambda}_n$, respectively, are roots of the equations

$$\sin(\lambda_n \beta) = \frac{1 - \nu}{3 + \nu} \lambda_n \sin \beta \tag{6a}$$

and

$$\sin(\bar{\lambda}_n \beta) = -\frac{1 - \nu}{3 + \nu} \bar{\lambda}_n \sin \beta. \tag{6b}$$

Eqs. (5a) and (5b) were developed by taking advantage of the symmetry of the corner with two free edges. The superscripts "A" and "S" in Eqs. (5a) and (5b) denote antisymmetric and symmetric corner functions, respectively. Accordingly, $W_c(r, \theta)$ in Eq. (3) may be expressed as

$$W_c(r, \theta) = \sum_{n=1}^N b_n W_{cn}^S(r, \theta) + \sum_{k=1}^K c_k W_{ck}^A(r, \theta). \tag{7}$$

The (r, θ) coordinate system is that shown in Fig. 2, where the origin (O) of the coordinate system is at the vertex of the V-notch, and the V-notch is symmetrical with respect to $\theta = 0$. If the corners A and B in Fig. 2 are the intersections of two free edges, no corner functions are needed at these points because these two

Table 1
Convergence of frequency parameters $\omega a^2 \sqrt{\rho/D}$ for a free square plate

Mode no.	Leissa [5]	Filipich and Rosales [6]	Order of polynomial ($I \times J$) in present solution							
			3 × 3	4 × 4	5 × 5	6 × 6	7 × 7	8 × 8	9 × 9	10 × 10
1	13.49	13.47	14.20	13.66	13.66	13.47	13.47	13.47	13.47	13.47
2	19.79	19.61	22.45	22.45	19.73	19.73	19.60	19.60	19.60	19.60
3	24.43	24.28	30.59	30.59	24.54	24.54	24.27	24.27	24.27	24.27
4	35.02	34.82	41.57	39.23	35.61	35.29	34.81	34.80	34.80	34.80
5	35.02	34.82	41.57	39.23	35.61	35.29	34.81	34.80	34.80	34.80

corner angles are less than 180° and all stresses are zero there during the vibration. The relations between (x, y) and (r, θ) coordinates are

$$r = [(x - c)^2 + (-y + b - d)^2]^{1/2}, \quad (8a)$$

$$\theta = \tan^{-1}[(x - c)/(-y + b - d)], \quad (8b)$$

where b, c and d are defined in Fig. 2.

Substituting Eqs. (3), (4) and (6a and b) into Eqs. (1a and b) and (2) and minimizing the functional Π with respect to the undetermined coefficients a_{ij} , b_n and c_k yields $I \times J + N + K$ algebraic linear equations for those undetermined coefficients, which results in an eigenvalue problem with the eigenvalues related to the natural frequencies of plate. To accurately solve the eigenvalue problem, variables with 128-bit precision (with approximately 34 decimal digit accuracy) were used in the developed computer program. However, one should recognize that as the number of functions is large, the matrices may become ill-conditioned, which causes numerical difficulties in accurately solving the eigenvalue problem.

3. Convergence studies

The Ritz method always provides upper-bound solutions for vibration frequencies, and the upper-bound solutions will converge to the exact solution as the number of admissible functions is sufficiently large and if the used admissible functions are from a mathematically complete set of functions. Convergence studies were carried out for completely free square plates with different notch depths and notch angles to verify the accuracy of the solutions and demonstrate the effects of corner functions on the solutions. The free plate uses $l = m = n = q = 0$ in Eq. (3). For simplicity, the same numbers of symmetric and antisymmetric corner functions ($N = K$ in Eq. (7)) were used. The numerical results for the first five nondimensional frequency parameters $\omega a^2 \sqrt{\rho/D}$, where a is a side length of the plate shown in Fig. 2, are given in the following tables for free, square plates with Poisson's ratio equal to 0.3. A V-notch was taken at $c/a = 0.5$. Notably, the first three rigid-body modes (zero frequencies) are not shown.

For comparison, Table 1 shows the convergence study of nondimensional frequency parameters for an intact (no notch) square plate, in which no corner functions were needed. The results do converge as upper bounds to the solutions, exact to the four significant figures shown as the number of admissible polynomial functions ($I \times J$) increases from 3×3 to 8×8 . Notably, the frequencies for the 4th and 5th modes are exactly the same, which are repeated eigenvalues in this eigenvalue problem when $b/a = 1$. The present results agree well with those determined by Leissa [5], who used 6×6 beam functions as admissible functions in the Ritz method. Since the beam functions may not form a complete set of functions, the converged results of Leissa [5] are larger than the present ones. Table 1 also shows that frequencies obtained by Filipich and Rosales [6], who utilized a whole element

method, are slightly less accurate than the converged values of the present method, the latter being exact to four digits. Table 1 establishes the accuracy of the computer program developed in the present study for the solutions without corner functions.

To further demonstrate the accuracy of the method using polynomials and corner functions as admissible functions, a convergence study was performed for a square plate with a very shallow V-notch ($d/b = 0.03$) having large notch angle $\alpha = 170^\circ$ that causes weak stress singularities at the vertex of the notch. The admissible functions of polynomials, which form a complete set of functions, are expected to give convergent results without numerical difficulties. Table 2 summarizes the convergence of frequency parameters $\omega a^2 \sqrt{\rho/D}$ by using polynomials and corner functions as admissible functions. As expected, the polynomial admissible functions give good convergent results. Adding corner functions into the admissible functions only slightly accelerates the convergence of the numerical solutions for this very shallow, wide angle notch.

Tables 3–5 list the convergence of frequency parameters $\omega a^2 \sqrt{\rho/D}$ for free, square plates with a V-notch having two different notch angles ($\alpha = 5^\circ$ or 30°) and depths ($d/b = 0.1$ or 0.5). The V-notch is much sharper than that considered in Table 2; and the corner functions are expected to have significant effects on the convergence of the solutions. In these cases under study, the admissible algebraic polynomials used alone give solutions with very slow convergence, especially for the case with a sharper ($\alpha = 5^\circ$) or deeper ($d/b = 0.5$) notch. Supplementing the admissible functions with corner functions significantly accelerates the convergence of the solutions.

In the case of the plate having a deep ($d/b = 0.5$), sharp ($\alpha = 5^\circ$) notch, Table 5 shows that the addition of corner functions is extremely important to obtain accurate frequencies. The accuracy of numerical results are dramatically improved by adding only one symmetric and antisymmetric corner functions that result in the singularities of moments at the vertex of the V-notch. For the first four frequencies shown, more accurate (i.e. better convergent) frequencies are obtained using only nine algebraic polynomial terms (3×3) and 10 corner functions ($K = N = 5$), resulting in an eigenvalue (frequency) determinant of order 19, than in the largest (9×9) polynomial solution with no corner functions. In the latter case one has a determinant of order 81.

There are two main reasons for the corner functions having such dramatic effects on the convergence of the numerical solutions. One is that the corner functions appropriately describe the singular behaviors of bending moments and transverse shear forces around the tip of the notch. Another is that the corner functions clearly and explicitly indicate the existence of the V-notch in the problems under consideration. When only the polynomial admissible functions are used in the Ritz method, the recognition of the existence of the V-notch is only through the integration domain. As the notch angle or the notch depth becomes smaller, the resulting integration domain is only slightly different from that without a V-notch. Thus, the corner functions satisfying the free edge conditions along the edges of a V-notch

Table 2
Convergence of frequency parameters $\omega a^2 \sqrt{\rho/D}$ for a free square plate with a V-notch ($c/a = 0.5$, $d/b = 0.03$, $\alpha = 170^\circ$)

Mode no.	No. of corner functions (K and N)	Order of polynomial ($I \times J$) in W_p						
		3×3	4×4	5×5	6×6	7×7	8×8	9×9
1	0	14.17	13.64	13.64	13.44	13.44	13.44	13.44
	1	14.17	13.62	13.61	13.44	13.44	13.44	13.44
	2	14.17	13.60	13.59	13.44	13.44	13.44	13.44
	3	14.10	13.60	13.51	13.44	13.44	13.44	13.44
2	0	22.87	22.87	20.05	20.05	19.91	19.91	19.91
	1	21.91	21.85	20.03	20.03	19.91	19.91	19.91
	2	21.86	20.98	20.03	20.03	19.91	19.91	19.91
	3	20.26	20.18	20.03	20.02	19.91	19.91	19.91
3	0	30.57	30.57	24.51	24.51	24.22	24.22	24.22
	1	28.95	28.85	24.46	24.46	24.22	24.22	24.21
	2	28.94	26.19	24.46	24.45	24.22	24.22	24.21
	3	28.94	25.28	24.42	24.38	24.22	24.22	24.21
4	0	41.42	39.05	35.56	35.21	34.75	34.74	34.74
	1	40.43	38.44	35.50	35.21	34.74	34.74	34.74
	2	40.04	37.88	35.45	35.20	34.74	34.74	34.74
	3	39.44	35.71	35.43	34.93	34.74	34.74	34.74
5	0	41.86	39.62	35.82	35.52	34.98	34.97	34.97
	1	41.32	38.48	35.65	35.35	34.97	34.97	34.97
	2	40.42	38.40	35.57	35.35	34.97	34.97	34.97
	3	40.42	37.28	35.44	35.30	34.97	34.97	34.97

Table 3
Convergence of frequency parameters $\omega a^2 \sqrt{\rho/D}$ for a free square plate with a V-notch ($c/a = 0.5$, $d/b = 0.1$, $\alpha = 30^\circ$)

Mode no.	No. of corner functions (K and N)	Order of polynomial ($I \times J$) in W_p						
		3×3	4×4	5×5	6×6	7×7	8×8	9×9
1	0	14.18	13.64	13.64	13.45	13.45	13.45	13.45
	3	13.73	13.47	13.47	13.30	13.30	13.30	13.30
	5	13.54	13.46	13.39	13.30	13.30	13.30	13.30
	7	13.50	13.42	13.31	13.30	13.30	/	/
2	0	22.55	22.55	19.81	19.81	19.67	19.67	19.67
	3	20.92	20.88	19.63	19.63	19.52	19.52	19.52
	5	20.61	19.88	19.62	19.62	19.52	19.52	19.52
	7	19.66	19.66	19.62	19.54	19.52	/	/
3	0	30.56	30.56	24.51	24.51	24.23	24.23	24.23
	3	28.77	27.97	24.31	24.31	24.06	24.06	24.06
	5	26.26	24.44	24.25	24.25	24.06	24.06	24.06
	7	24.35	24.33	24.18	24.14	24.06	/	/
4	0	41.48	39.11	35.54	35.20	34.73	34.72	34.72
	3	39.17	36.24	34.88	34.63	34.17	34.16	34.16
	5	37.16	35.14	34.85	34.44	34.17	34.16	34.16
	7	35.56	34.84	34.79	34.21	34.17	/	/
5	0	41.70	39.37	35.70	35.38	34.88	34.87	34.87
	3	39.42	37.82	35.09	34.77	34.42	34.42	34.41
	5	38.25	36.15	34.99	34.74	34.42	34.41	34.41
	7	36.49	35.16	34.84	34.71	34.41	/	/

Note: “/” denotes no data available because of matrix ill-conditioning.

definitely help the formulation in the Ritz method in realizing the existence of the V-notch.

Table 3 displays that adding the corner functions into the admissible polynomials may yield ill-conditioned matrices at the

number of admissible functions not very large. Without showing the results, ill-conditioning also occurs when only the set of polynomial functions with I and J larger than 15 is used. The ill-conditioning is due to numerical roundoff errors. When the

Table 4Convergence of frequency parameters $\omega a^2 \sqrt{\rho/D}$ for a free square plate with a V-notch ($c/a = 0.5$, $d/b = 0.5$, $\alpha = 30^\circ$)

Mode no.	No. of corner functions (K and N)	Order of polynomial ($I \times J$) in W_p						
		3×3	4×4	5×5	6×6	7×7	8×8	9×9
1	0	13.72	13.09	13.09	12.80	12.80	12.72	12.72
	1	9.228	8.953	8.843	8.792	8.791	8.778	8.778
	5	8.808	8.773	8.759	8.726	8.725	8.725	8.725
	10	8.739	8.727	8.727	8.725	8.725	8.725	8.725
	15	8.734	8.726	8.726	8.725	8.725	8.725	8.725
2	0	23.35	23.32	20.33	20.32	19.98	19.98	19.76
	1	17.79	17.72	16.86	16.86	16.80	16.80	16.78
	5	17.00	16.95	16.80	16.80	16.76	16.76	16.76
	10	16.82	16.80	16.77	16.76	16.76	16.76	16.76
	15	16.81	16.79	16.76	16.76	16.76	16.76	16.76
3	0	30.18	30.11	23.89	23.88	23.30	23.30	23.07
	1	25.72	25.54	22.19	22.18	22.04	22.04	22.03
	5	24.14	23.36	22.17	22.16	22.01	22.01	22.01
	10	22.17	22.17	22.03	22.01	22.01	22.01	22.01
	15	22.12	22.12	22.02	22.01	22.01	22.01	22.01
4	0	40.41	37.48	34.23	33.45	33.11	32.90	32.90
	1	29.99	29.06	27.65	27.25	27.13	27.06	27.06
	5	28.73	27.46	27.35	27.14	27.01	26.99	26.99
	10	27.24	27.14	27.12	26.99	26.99	26.99	26.99
	15	27.13	27.08	27.02	26.99	26.99	26.99	26.99
5	0	44.28	41.79	37.49	37.19	36.30	36.29	36.07
	1	41.56	39.66	35.74	35.51	35.09	35.09	35.08
	5	38.83	36.87	35.60	35.37	34.99	34.98	34.98
	10	36.02	35.53	35.18	35.07	34.98	34.98	34.98
	15	35.82	35.24	35.00	34.99	34.98	34.98	34.98

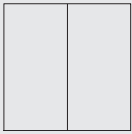
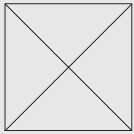
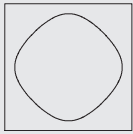
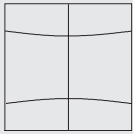
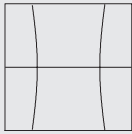
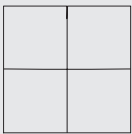
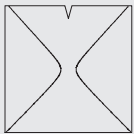
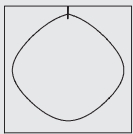
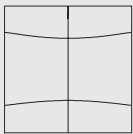
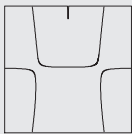
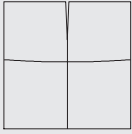
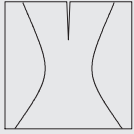
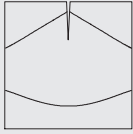
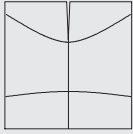
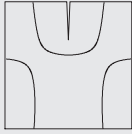
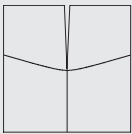
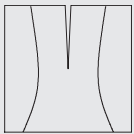
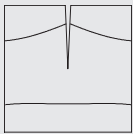
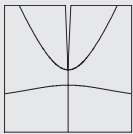
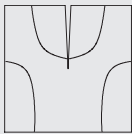
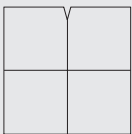
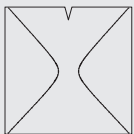
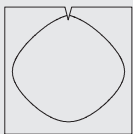
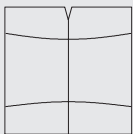
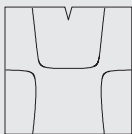
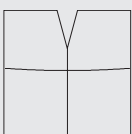
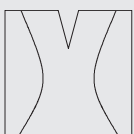
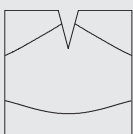
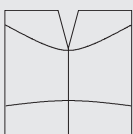
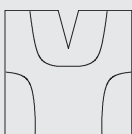
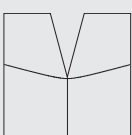
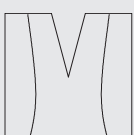
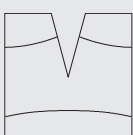
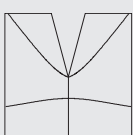
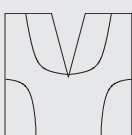
Table 5Convergence of frequency parameters $\omega a^2 \sqrt{\rho/D}$ for a free square plate with a V-notch ($c/a = 0.5$, $d/b = 0.5$, $\alpha = 5^\circ$)

Mode no.	No. of corner functions (K and N)	Order of polynomial ($I \times J$) in W_p						
		3×3	4×4	5×5	6×6	7×7	8×8	9×9
1	0	14.12	13.57	13.57	13.38	13.38	13.38	13.38
	1	8.882	8.646	8.542	8.501	8.500	8.493	8.493
	5	8.409	8.368	8.353	8.323	8.323	8.322	8.322
	10	8.335	8.323	8.323	8.322	8.322	8.322	8.322
	15	8.331	8.322	8.322	8.322	8.322	8.322	8.322
2	0	22.56	22.56	19.80	19.80	19.65	19.65	19.65
	1	15.96	15.89	15.25	15.25	15.20	15.20	15.19
	5	15.54	15.33	15.15	15.14	15.11	5.11	15.11
	10	15.18	15.14	15.11	15.11	15.11	15.11	15.11
	15	15.16	15.14	15.11	15.11	15.11	15.11	15.11
3	0	30.53	30.53	24.44	24.44	24.14	24.14	24.14
	1	25.90	25.24	22.20	22.20	22.02	22.02	22.02
	5	24.00	23.52	22.13	22.13	21.97	21.97	21.97
	10	22.12	22.12	21.99	21.98	21.97	21.97	21.97
	15	22.07	22.07	21.97	21.97	21.97	21.97	21.97
4	0	41.37	38.95	35.39	35.02	34.56	34.55	34.55
	1	26.09	26.03	24.54	24.18	24.13	24.07	24.07
	5	24.76	24.12	24.03	23.82	23.77	23.74	23.74
	10	23.99	23.84	23.81	23.74	23.74	23.73	23.73
	15	23.83	23.80	23.76	23.73	23.73	23.73	23.73
5	0	41.88	39.52	35.81	35.49	34.95	34.94	34.93
	1	38.60	36.98	33.11	32.88	32.49	32.49	32.49
	5	35.94	34.99	32.90	32.67	32.33	32.32	32.32
	10	33.14	32.86	32.68	32.49	32.33	32.32	32.32
	15	32.92	32.61	32.34	32.33	32.32	32.32	32.32

variables in a computer program are defined with less decimal digit accuracy, the ill-conditioning will occur at smaller number of admissible functions. It is known by many numerical analysts that using orthogonal algebraic polynomials, instead of the ordinary ones expressed in Eq. (4), may reduce ill-conditioning greatly. This would complicate the present analysis significantly. Nevertheless, results with good accuracy (four-digit convergence) were obtained for Table 3, using the present method, before the ill-conditioning occurred.

Tables 3–5 give some important findings. Comparing the results of Table 4 with those of Table 3, one finds that more corner functions are needed to get four-digit convergence solutions for a plate with a deeper V-notch when the same number of polynomial functions is used. Comparing the results of Tables 4 and 5, one sees that more corner functions may not be needed to get four-digit convergence solutions when the notch angle changes from $\alpha = 30^\circ$ to 5° . Moreover, an incorrect judgment on the convergent solutions may result if no corner

Table 6
Frequency parameters $\omega a^2 \sqrt{\rho/D}$ and nodal patterns for square plates with a V-notch at $c/a = 0.5$

α	d/b	Mode no.					
		1	2	3	4	5	
0°	0	 (13.47)	 (19.60)	 (24.27)	 (34.80)	 (34.80)	
	5°	0.1	 (13.30)	 (19.43)	 (24.08)	 (34.19)	 (34.27)
		0.3	 (11.58)	 (17.93)	 (22.88)	 (28.65)	 (32.53)
		0.5	 (8.322)	 (15.11)	 (21.97)	 (23.73)	 (32.32)
30°	0.1	 (13.30)	 (19.52)	 (24.06)	 (34.16)	 (34.41)	
	0.3	 (11.59)	 (18.68)	 (22.81)	 (29.45)	 (33.76)	
	0.5	 (8.725)	 (16.76)	 (22.01)	 (26.99)	 (34.98)	

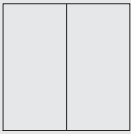
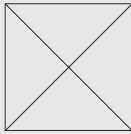
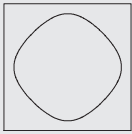

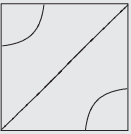
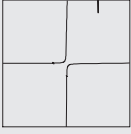
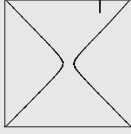
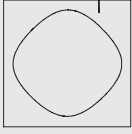
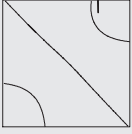
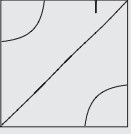
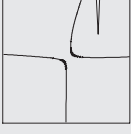
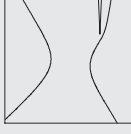
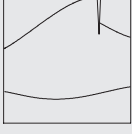
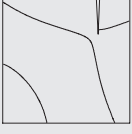
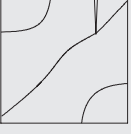
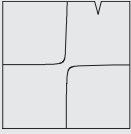
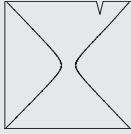
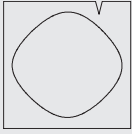
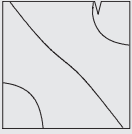
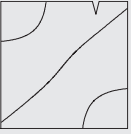

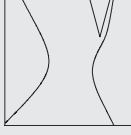
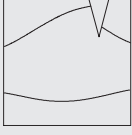
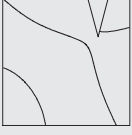
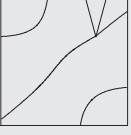
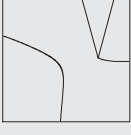

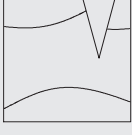
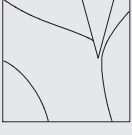

functions are involved in the admissible functions. For example, from the first row data in Table 5, one may conclude incorrectly that the converged value of $\omega a^2 \sqrt{\rho/D}$ is in the vicinity of 13.38, which is far greater than the accurate, converged values given (8.322).

4. Numerical results and discussion

Tables 6 and 7 display the nondimensional frequency parameters and corresponding nodal patterns (lines of zero vibration

displacement) of the first five nonzero frequency modes for free, square plates with a V-notch at two different locations and having different notch angles and notch depths. Poisson's ratio is set equal to 0.3. The results for a shallow notch ($d/b = 0.1$) were obtained by using 9×9 terms of polynomials along with 5 symmetric and antisymmetric corner functions, while the results for $d/b = 0.3$ or 0.5 were obtained by using 8×8 terms of polynomials and 15 symmetric and antisymmetric corner functions. Convergence studies show that the results have at least three-digit convergence.

Table 7
Frequency parameters $\omega a^2 \sqrt{\rho/D}$ and nodal patterns for square plates with a V-notch at $c/a = 0.75$

α	d/b	Mode no.				
		1	2	3	4	5
0°	0	 (13.47)	 (19.60)	 (24.27)	 (34.80)	 (34.80)
	0.1	 (13.37)	 (19.53)	 (24.21)	 (34.20)	 (34.67)
	0.3	 (12.15)	 (18.48)	 (22.87)	 (27.88)	 (34.09)
30°	0.1	 (13.39)	 (19.57)	 (24.23)	 (34.20)	 (34.77)
	0.3	 (12.40)	 (18.75)	 (23.09)	 (28.57)	 (34.91)
	0.5	 (9.714)	 (16.46)	 (21.91)	 (26.72)	 (35.02)

It is interesting to observe how the frequency parameters change with α , d/b and c/a . The frequency parameters, except for those for the fifth modes for $\alpha = 30^\circ$ and $d/b = 0.5$, significantly decrease as the notch depth d/b increases for V-notched square plates mainly because of significant reduction in the flexural stiffness for larger d/b , without significant reduction in mass. The decreasing frequencies relative to the frequencies of an intact (no notch) plate are considerably different for different modes. Interestingly, the frequency of the fifth mode for $\alpha = 30^\circ$, $d/b = 0.5$ and $c/a = 0.5$ or 0.75 is larger than that of an intact plate. The V-notched plates with $c/a = 0.5$ have larger decreasing rates than those for $c/a = 0.75$ in the first and fifth modes. When $d/b = 0.5$, the frequency parameters increase if α changes from 5° to 30° . This trend is also generally observed with few exceptions in the cases of $d/b = 0.1$ and 0.3 . The frequency parameters for the first and fifth modes increase as c/a changes from 0.5 to 0.75 .

Before discussing the effects of α , d/b and c/a on the nodal patterns, one may note that the nodal patterns of the fourth and fifth modes for an intact square plate are shown differently in Table 6 than in Table 7. The nodal patterns given in both tables are correct because the frequencies for these two modes are identical. Mathematically, when an eigenvalue problem has two repeated eigenvalues, any linear combination of the corresponding eigenfunctions is also a possible eigenfunction. Consequently, there are an infinite number of possible combinations of the fourth and fifth mode shapes for an intact square plate. The mode shapes given in these tables for the intact plate are thus chosen because they are often seen in published literature and they resemble those for a square plate with a shallow V-notch.

Tables 6 and 7 also reveal that the nodal patterns for the shallow notch ($d/b = 0.1$), at first sight, look very similar to those for an intact square plate (i.e., $d/b = 0$), respectively. However, if observing carefully, one can find some significant differences. A V-notch at $c/a = 0.5$ destroys the symmetry about the horizontal axis, and the notch at $c/a = 0.75$ destroys the symmetry about all axes. The crossing nodal lines for $d/b = 0$ may separate when a V-notch exists (i.e., the second and fifth modes in Table 6 and the first and second modes in Table 7). A straight nodal line for $d/b = 0$ may be distorted when a V-notch exists (i.e., the horizontal nodal line of the first mode in Table 6 and the diagonal nodal lines of the fourth and fifth modes in Table 7).

When d/b changes from 0.1 to 0.3 and to 0.5 , the nodal patterns change significantly. The curve veering and the distortion of the straight nodal lines become more significant as α or d/b increases. The almost closed nodal line in the third mode is destroyed drastically when d/b changes from 0.1 to 0.3 to 0.5 . Changing d/b does not result in changes in modal order for similar nodal patterns.

Let us now return to a question asked in the Introduction to this work: "Can a shallow notch cause significant changes in the plate natural frequencies and mode shapes?" Looking at the results in Tables 6 and 7 for a shallow notch having $d/b = 0.1$, one finds that the maximum change in frequency from that of an intact plate ($d/b = 0$), at least among the first five frequencies, is 1.8 percent. This occurs in the fourth mode of the centrally notched ($c/a = 0.5$) plate with $\alpha = 30^\circ$ (Table 6). Looking at the nodal patterns for the shallow notches in Tables 6 and 7, one sees that their changes from those of the intact plate are small, except in some cases where the notch causes lines to lose their symmetry, and separate instead of crossing.

5. Conclusions

This paper has presented a method to accurately determine the natural frequencies of plates having V-notches along their edges. This method is laid out in detail for rectangular plates

having a single V-notch. Using the Ritz method, convergence of the numerical solutions is accelerated by supplementing the regular polynomial admissible functions with the corner functions that are the fundamental solutions of the bi-harmonic plate equation, exactly satisfy the free boundary conditions along the V-notch, and properly describe the bending moment and shear force singularities at the neighborhood of the tip of V-notch. The effects of the corner functions on determining the frequencies of a plate were comprehensively investigated through careful convergence studies for plates with different notch depths and angles. When the notch angle (α) becomes smaller, the corner functions are necessary to achieve accurate solutions.

Accurate numerical results and nodal patterns have been tabulated for V-notched, completely free, square plates having notch angle $\alpha = 5^\circ$ or 30° at different locations and with various notch depths. The numerical results shown are exact to at least three significant figures. These are the first known frequency and nodal pattern results available in the published literature. A deep V-notch significantly alters the nondimensional frequency parameters and the nodal patterns of V-notched plates. But it is shown that a shallow V-notch has only a small effect upon the vibration frequencies and nodal patterns, in spite of the very high bending stresses that arise in the vicinity of the vertex of the notch. The reliable results shown here serves not only to improve the understanding of the vibration behavior of a V-notched square plate, but also as benchmark data against which other numerical methods may be checked.

Although numerical results are given here only for V-notched square plates with free boundary conditions, the methodology used here can be easily extended to investigate the vibration behavior of V-notched plates with different shapes and various boundary conditions. It will be more challenging to apply the present methodology to study the behaviors of a plate with a cut-out because there will then be more than one corner having stress singularities.

The present approach cannot be directly applied to solve problems with a side crack. For this a special analysis must be made. When $\alpha = 0$ (a crack), the roots of Eqs. (6a and b) are λ_n or $\bar{\lambda}_n$ equal to $n/2$ and $n = 1, 2, 3, \dots$. When λ_n or $\bar{\lambda}_n$ are integers, the corresponding corner functions may depend linearly on the polynomial admissible functions and cause numerical difficulties in solving the resulting eigenvalue problem. Furthermore, when $\bar{\lambda}_n$ is not an integer, $\cos[(\bar{\lambda}_n - 1)\beta/2]$ and $\cos[(\bar{\lambda}_n + 1)\beta/2]$ in Eq. (5b) are equal to zero. Consequently, Eq. (5b) cannot be directly used. How to apply a similar approach to solve a problem with an edge crack will be investigated in another paper.

References

- [1] Leissa AW. Vibration of plates. NASA SP-160, 1969. [Reprinted, Acoustical Society of America; 1993.]
- [2] Williams ML. Surface stress singularities resulting from various boundary conditions in angular corners of plates under bending. In: Proceedings of the First US National Congress of applied mechanics, 1952. p. 325–329.
- [3] Leissa AW, McGee OG, Huang CS. Vibrations of sectorial plates having corner stress singularities. Journal of Applied Mechanics 1993;60:134–40.
- [4] Leissa AW, McGee OG, Huang CS. Vibrations of circular plates having V-notches or sharp radial cracks. Journal of Sound and Vibration 1993;161(2): 227–39.
- [5] Leissa AW. The free vibration of rectangular plates. Journal of Sound and Vibration 1973;31(3):257–93.
- [6] Filipich CP, Rosales MB. Arbitrary precision frequencies of a free rectangular thin plate. Journal of Sound and Vibration 2000;230(3):521–39.